Earth and Environmental Science Transactions of the Royal Society of Edinburgh, **103**, 237–250, 2013 (for 2012)

Histological characteristics of the vertebral intercentra of *Metoposaurus diagnosticus* (Temnospondyli) from the Upper Triassic of Krasiejów (Upper Silesia, Poland)

D. Konietzko-Meier[1,2], A. Bodzioch[2] and P. M. Sander[1]

[1] Steinmann Institute, Division of Paleontology, University of Bonn, Nussallee 8, 53115 Bonn, Germany.
Email: Martin.Sander@uni-bonn.de

[2] Department of Biosystematics, University of Opole, Oleska 22, 45-052 Opole, Poland.
Email: Dorota.Majer@uni.opole.pl; abodzioch@uni.opole.pl

ABSTRACT: Osteohistological characteristics of the large temnospondyl amphibian *Metoposaurus diagnosticus* from the Upper Triassic of Poland (Krasiejów locality) were determined using vertebral intercentra thin-sections from different regions and growth stages. The intercentra showed a trabecular structure in both the endochondral and periosteal domains. Endochondral ossification developed first, and the primary bone occurs near the periphery with a higher degree of remodelling in the centre. Periosteal bone deposition begins later; first on the ventral side, continuing laterally and finally onto the dorsal side. Periosteal growth rate was initially very rapid, and then subsequently decreased in rate. In all sections, numerous remains of calcified cartilage are visible, which may indicate a juvenile, paedomorphic or plesiomorphic character. The four histologic ontogenetic stages (HOS) of sampled vertebrae were determined based on growth marks. Most of the sampled bones belong to juvenile individuals (HOS 1 to 3), apart from one atlas and the largest anterior dorsal intercentrum, which represent the oldest described stage (HOS 4). Sharpey's fibres are preserved in ventro-lateral cortical regions, around parapophyses and on the posterior side of the neural arch.

KEY WORDS: cartilage, HOS, morphogenesis, paedomorphosis, palaeohistology.

Osteohistology of fossil reptiles, especially dinosaurs, is well studied, while the literature about the palaeohistology of large temnospondyl amphibians is still scant (e.g. Gross 1934; Enlow & Brown 1956; de Ricqlès 1975, 1976, 1978, 1979, 1992; Damiani 2000; de Ricqlès *et al.* 2004; Steyer *et al.* 2004; Ray *et al.* 2009; Mukherjee *et al.* 2010; Sanchez *et al.* 2010a, b, c). Moreover, the studied material tended to be non-diagnostic and usually non-homologous elements were examined. Long bones are often studied and data on the dermal skeleton has been recently presented (e.g. Witzmann 2009; Witzmann & Soler-Gijón 2010). Histological descriptions of temnospondyl amphibian vertebrae are extremely rare (Mukherjee *et al.* 2010), although the vertebral column forms an important part of whole skeleton, and vertebrae are one of the most numerous and common fossil remains (de Buffrénil *et al.* 1986).

The main goal of this study was to document the microanatomy and histology of metoposaur intercentra and to interpret the osteogenic processes involved in the vertebral growth using histological methods. Also, using the histological information, we can infer some ideas about life history.

Institutional abbreviations. UOBS (old catalogue system) and UOPB (new catalogue system): University of Opole, Department of Biosystematics, Poland.

1. Material and methods

1.1. Material

1.1.1. Locality. The vertebrae of *Metoposaurus diagnosticus* studied here come from the Late Triassic famous locality of Krasiejów, western part of Upper Silesia, Opole region, Poland. Two horizons of fine-grained, alluvial deposits have yielded amphibian and reptilian material (see Dzik *et al.* 2000; Sulej 2002; Dzik & Sulej 2007; Szulc 2007 for details of palaeofauna, geographical and geological setting).

1.1.2. Species and axial-regional determination. Two temnospondyl taxa are known from the Krasiejów locality; *Metoposaurus diagnosticus krasiejowensis* Sulej, 2002 and *Cyclotosaurus intermedius* Sulej & Majer, 2005. For species identification, the shape of the studied intercentra (*Metoposaurus* vs. *Cyclotosaurus*) is used: in *Metoposaurus*, they are round and fully ossified, while in *Cyclotosaurus*, only the ventral part of the vertebra is ossified and the intercentrum has a very characteristic crescent shape (Dzik *et al.* 2000). In this paper, we describe only material assignable to *Metoposaurus diagnosticus krasiejowensis*.

The studied specimens belong to the huge collection of isolated bones from the Opole University are: two atlases with neural arches; one post-cervical; four anterior dorsal; three mid-dorsal; one presacral; two postsacral; one anterior caudal; and one posterior caudal vertebrae (Table 1). All intercentra were disarticulated, and the axial-regional distinction between them was made on the basis of characteristics described by Sulej (2007). However, their precise position in the specific region in the vertebral column, except for atlas, was not possible to determine.

The shape of the intercentrum of the atlas is more oval than the others (Fig. 1A–E). On the anterior surface, two facets that articulate with the occipital condyles are present. The posterior side is concave, forming a single, transversely elongated oval. The neural arch is permanently fused with the intercentrum (Sulej 2007). The other vertebrae show a large, characteristic circular intercentrum with laterally located parapophyses used for articulation with the tuberculum of ribs (Fig. 1F–J).

The details about the morphology of each vertebral region, including photographs, are given in the Sulej (2007) paper. In the postcervical intercentra, the parapophyses are large and

 doi:10.1017/S1755691013000273

Table 1 Position, cutting plane, size, relative size, HOS and estimated ontogenetic stages of examined intercentra of *Metoposaurus diagnosticus krasiejowensis* from the Late Triassic of Poland.

number	position	cutting plane	length[1] (mm)	height (mm)	width (mm)	% max. width[2]	% max. estimated size[3]	class-size/ HOS[4]	estimated ontogenetic stage
UOBS 00859	atlas with neural arch	transverse and horizontal on the basis of the neural arch	23·5	32·0*	42·3*	46	38	II/2	juvenile
UOPB 00012	atlas with neural arch	sagittal	20	40·0*	51·2*	56	46	III/4	sub-adult
UOPB 01014	post-cervical	transverse	21·2	26·2	33·1	70	30	II/2	juvenile
UOPB 00117	anterior dorsal	sagittal	12·4	17·9	20·1	28	17	I/1	early juvenile
UOPB 01010	anterior dorsal	sagittal	21·7	32·7	40·7	57	36	II/2	juvenile?
UOPB 00115	anterior dorsal	sagittal	22·5	44·5	52	73	47	III/3	late juvenile
UOPB 00114	anterior dorsal	sagittal	36	56·5	71	100	64	IV/4	sub-adult
UOPB 01019	mid-dorsal	horizontal	23·2	32·1	41·5	62	37	II/?	?
UOPB 01018	mid-dorsal	horizontal	23	35	43	64	38	II/?	?
UOPB 01017	mid-dorsal	sagittal	22·6	36·8	44·7	67	40	II/2	juvenile
UOPB 00118	presacral	sagittal and transverse	21	41	59	83		/3	late juvenile
UOPB 01008	postsacral	transverse	14·5	23·8	33·6	84		/2	juvenile
UOPB 01011	postsacral	sagittal	19	28·6	36·8	92		/2	juvenile
UOPB 01005	anterior caudal	sagittal	22·3	29·5	31·5	92		/2	juvenile?
UOPB 01004	posterior caudal	transverse	21·5	22·8	30	73		/2	juvenile

* Measurements of the posterior face of the axis without high of neural arch

[1] the position of the measurement marked on Fig. 2

[2] Percent of the width of the largest known vertebra from this position (from Sulej 2007, except UOPB 00114)

[3] Percent of the width of the largest estimated intercentrum (on the basis of the width of both occipital condyles from the largest known skull, from Sulej 2007 – see section 1.2.2.

[4] Histologic Ontogenetical Stage

– The identification of the ontogenetic stage is either not possible (because of the plane of cutting – horizontal in mid-dorsal vertebra) or uncertain (because of the preservation of the cortex in the anterior caudal vertebrae)

x–The estimation for the maximal estimated size is impossible for the regions further than perisacral (for details see section 1.2.2).

longer than half of the length of the lateral surface of intercentra. The anterior surface and ventral edge are convex in ventral view; the posterior side is concave (Sulej 2007).

In the anterior dorsal region of the vertebral column, intercentra have parapophyses longer than half of the lateral length, with a flat anterior surface and a concave posterior surface (Fig. 1L). In the mid-dorsal intercentra (Fig. 1M), the parapophyses are shorter and the anterior and posterior surfaces of intercentrum are flat or slightly concave (Sulej 2007).

Vertebrae belonging to the perisacral region may be distinguished into two morphotypes. The first one, termed "presacral" by Sulej (2007) or "thoracic" by Dutuit (1976), has small and very short anterior and posterior parapophyses. There is a sharp notch which lies between the medial edge of the posterior parapophyses and the posterior facet of articulation. The intercentrum has slightly concave anterior and posterior surfaces (Fig. 1M). Typically, *Dutuitosaurus* has only three (Dutuit 1976) or four (Sulej 2007) perisacral vertebrae. The posterior parapophysis of perisacral vertebrae is much shorter and the anterior one is larger than in the presacral vertebrae. Functionally, the postsacral vertebrae (Fig. 1O) belong to the caudal vertebrae, but the morphological framework (lack of chevron) is more similar to the perisacral region than to the typical caudal region (Dutuit 1976; Sulej 2007). The posterior and anterior parapophyses are similar in size, and are very close to each other. Both parapophyses are positioned very low and have an almost flat ventral surface, which is characteristic of this type of intercentrum (Sulej 2007).

The chevrons are fused with the intercentra in the caudal region (Fig. 1P). The intercentra from the anterior caudal region are trapezoidal in lateral view, and the posterior caudal region differs from the previous intercentra as they are triangular in lateral view. The intercentra bear small and vertically elongated, or large and rounded parapophyses (Sulej 2007).

1.2. Methods

1.2.1. Histological sections. The bones were prepared by mechanically removing slightly cemented clay and washing them in clear water. Thin sections were cut out along three mutually perpendicular planes: sagittal, transverse and horizontal, going through the geometric centre of an intercentrum (Fig. 2). Each intercentrum has been cut at least once and at most twice (Table 1). The sections were prepared in the laboratory of the Division of Palaeontology (Steinmann Institute, University of Bonn) and in the Institute of Geology at the A. Mickiewicz University, Poznań, according the standard procedure (i.e. Enlow & Brown 1956; Wells 1989; Chinsamy & Raath 1992). The vertebrae were embedded in polyester resin that cures water-clear and cut along the axis described in Table 1. The freshly cut surfaces were impregnated with resin in a vacuum chamber to reduce the risk of air bubbles that may obscure the slide. The sectioned surfaces were ground with wet SiC grinding powder in the sequence of 400, 600 and 800 grit sizes. Once the embedded surface was smooth enough, it was glued with resin onto a frosted glass slide of the desired size and left to dry. Then, a sample was cut to a thickness of a few millimetres, using an automatic rock saw, and further manually ground with the series of wet SiC powder to a thickness of about 90 to 80 μm. The desired thickness can be approximated by repeated control with a polarising microscope. Finally, a cover slip was put on the section to increase the contrast and protect the sample.

The thin sections were studied under a LEICA DMLP light microscope in normal and polarised light in magnification ranges from 25 to 400. The photos were taken by the Leica DFC 420 camera attachment for the microscope. The histological terminology follows Francillon-Vieillot *et al.* (1990) and the morphology description follows Sulej (2007).

https://doi.org/10.1017/S1755691013000273 Published online by Cambridge University Press

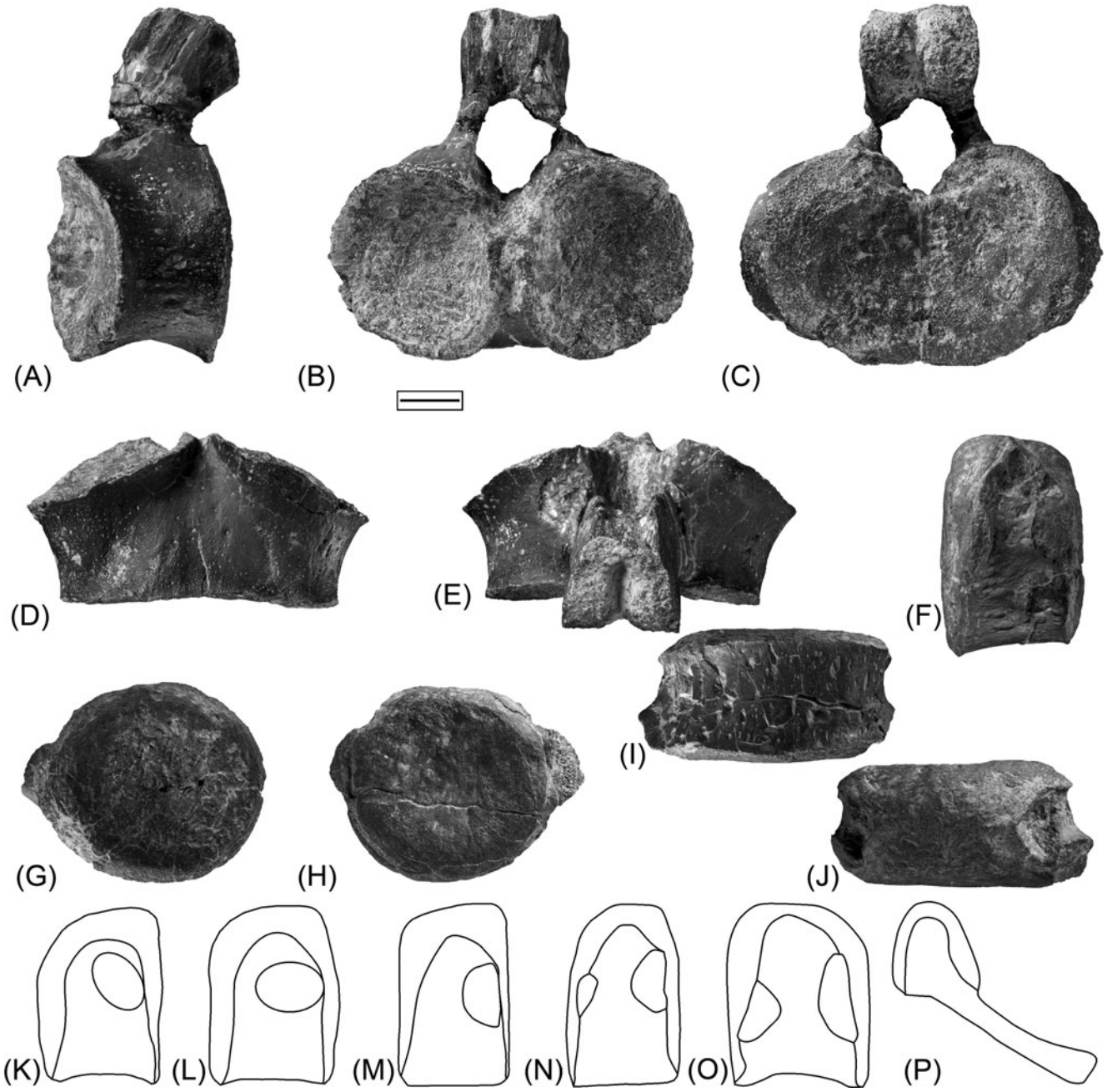

Figure 1 General morphology of the atlas and a presacral intercentrum of *Metoposaurus diagnosticus krasiejowensis* from the Late Triassic of Poland: (A–E) atlas (UOPB 00013) in left lateral (A), anterior (B), posterior (C), ventral (D) and dorsal (E) views; (F–J) presacral intercentrum (UOPB 00119) in left lateral (F), anterior (G), posterior (H), ventral (I) and dorsal (J) views; (K–P) drawings of left lateral views of the vertebrae from postcervical (K), anterior dorsal (L), mid-dorsal (M), presacral (N), postsacral (O) and anterior (P) caudal regions. Note the different positions and size of the parapophyses. Scale bar (A–J) = 1 cm.

1.2.2. Analysis. The disarticulated state of the sampled material generates difficulties for interpreting and correlating the size in each type of vertebrae. The difference in size between the intercentra from similar regions may be a result of real differences in age, but also the individual variability i.e. the growth rate of each individual or the position in the vertebral column.

The reconstruction of the vertebral column of *Metoposaurus diagnosticus krasiejowensis* presented in Sulej (2007, fig. 72B–D) is composed on the basis of few sources; the articulated fragments of postcervical (ZPAL AbIII/1132/1), anterior dorsal (ZPAL AbIII/1133/1) and caudal regions (ZPAL AbIII/1189) of the vertebral column from Krasiejów (Sulej 2007, figs 31, 35), the *Metoposaurus diagnosticus diagnosticus* (SMNS 5143) from the Schilsandstein of Württemberg and mainly on the articulate skeletons of *Dutuitosaurus ouazzoui* from the Argana Formation of Morocco. Therefore, the articulated and complete skeletons of *Dutuitosaurus ouazzoui* were used additionally as a proxy in the cross-scaling between the sizes of vertebrae in the current study. In the *Dutuitosaurus ouazzoui* (Dutuit 1976, panels: XXX–XXXIV and personal observation of specimens in the collections of the Muséum National d'Histoire Naturelle, Paris by the first author), the width of the intercentra, from the atlas to the perisacral region, is rather uniform and fixed for each growth stage. The few articulated specimens of *Metoposaurus* listed above confirm the same tendency in Krasiejów taxon.

Moreover, the width of the atlas and of both occipital condyles is directly related. Based on the width of the occipital condyles of the largest isolated skull from Krasiejów, presenting

https://doi.org/10.1017/S1755691013000273 Published online by Cambridge University Press

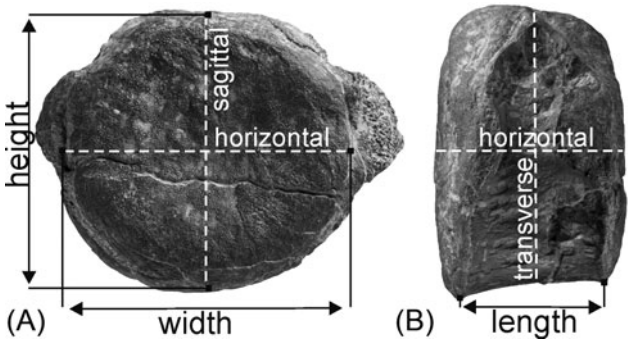

Figure 2 Measurement positions and cutting planes of the vertebrae of *Metoposaurus diagnosticus krasiejowensis* from the Late Triassic of Poland: (A) presacral intercentrum in posterior view; (B) the same intercentrum in left lateral view.

a well preserved occipital region (ZPAL AbIII/1192 – 470 mm the length of skull roof; Sulej 2007), the width of the largest atlas has been estimated. As described above, the regularity in the vertebrae size along the vertebral column allows us to estimate the maximal size for successive intercentra from atlas to perisacral region (Table 1). Therefore, comparison of the width of the estimated largest known atlas with the width of the studied intercentra allows us to compare ontogenetic development of the atlas with other vertebrae.

A single growth series was determined for the four anterior dorsal intercentra using the *Dutuitosaurus* specimen and the reconstruction of the *Metoposaurus* skeleton, plus the vertebrae of the current study. The width of the smallest intercentra was only 28·25% that of the largest studied (Table 1). In the dorsal region, the intercentra are rather similar in width but the large size distinction (about 80%) may suggest an ontogenetic influence. Also, the histological data show the different histological framework for each vertebra (for details see section 2.2.4). On the basis of that growth series, a preliminary analysis of growth processes and an ontogenetic stage estimation were possible for atlases, anterior-dorsal and mid-dorsal vertebrae. On the basis of histological features, four histological ontogenetic stages (HOS were erected: HOS 1 – early juvenile; HOS 2 – juvenile; HOS 3 – late juvenile; HOS 4 – older than late juvenile). The best growth characters are visible in the ventral part of the cortex, and therefore, the determination was not possible in specimens cut in a horizontal plane (two mid-dorsal intercentra).

2. Results

2.1. General description

2.1.1. Microanatomy. The variability of the microanatomical and histological pattern of the intercentra, from the anterior to posterior part of vertebral column, is very low. The entire intercentra are derived from trabecular bone (Fig. 3).

Independently from the ontogenetic stage, the anterior and posterior faces of the intercentrum (Fig. 3A, D, E) and the floor of the neural arch always have endochondral bone (Fig. 3C, F). In the remaining part of the intercentrum, the endochondral trabecular bone reaches the edge of the bone or is surrounded by a periosteal cortex, depending on the ontogenetic stage.

In the transverse sections, the periosteal bone occurs mostly along the ventral and lateral surfaces, and also below and under the parapophyses. In two specimens, atlas (UOBS 00859) and presacral (UOPB 00118), the periosteal bone is present also on the dorsal side, with the exception of the neural canal region (Fig. 3C, F). In sagittal view, the periosteal bone is shaped like a triangle (Fig. 3D). In all the specimens, the apex of this triangle is ventral to the geometrical centre of section, except in the largest anterior dorsal intercentrum (UOPB 00114) where the apex is higher than the central point (Fig. 3D).

The border between endochondral and periosteal domains is visible as an oblique line, sharper near the surface, and gradually disappears toward the central part of the centrum (Fig. 3D). The limit between the periosteal and endochondral bone is marked by a different orientation of the trabeculae. In the periosteal bone, the trabeculae consist of a very regular net, parallel to the surface of the intercentrum. In the endochondral bone, the trabeculae build an irregular net, without particular orientation (Fig. 3C, D, F).

2.1.2. General histology. The whole intercentrum shows highly trabecular structures, periosteal, endochondral and secondary ossification (Fig. 4).

The periosteal cortex is highly vascularised, with a parallel-fibred matrix (Fig. 4A–D). The vascular system forms a dense, layered network in the cortex. The vascular canals are oriented parallel to the external surface of the cortex, in the anteroposterior axis. Inside most of these canals, the primary deposition of lamellar bone is visible (e.g. Fig. 4C). Poorly vascularised lamellar bone patches are visible around parapophyses in transverse sections (e.g. Fig. 7B). The lamellar layers are also visible in the annuli on the ventral part of some intercentra (Figs 4E–G, 6E–H, 7C–E). However, in all specimens, the well preserved organisation of periosteal cortex is visible in the thin, external layer. In the inner part of the cortex, the large erosion cavities are present and randomly arranged bone trabecluae are visible (e.g. Fig. 4C). The periosteal bone gradually changes to the endochondral bone through secondary trabeculae without, or almost without, calcified cartilage, with concentric or half rings of lamellae which sometimes cover each other (Fig. 4I). The number of generations of the visible half rings reaches a maximum of three. In the remodelled part, the typical secondary osteons are very rare. Leading to the dorsal, anterior and posterior surfaces, an irregular network of thin endochondral bony trabeculae are present, separated by large pore spaces. Trabecular bone dominates and remains of calcified cartilage between trabeculae are more numerous (Fig. 4J, K). Large remains of cartilage cover the whole anterior and posterior articulate surface of the intercentra and the floor of the neural canals (Fig. 4H).

Osteocyte lacunae are mostly round (Fig. 4B), except in the external annuli where they are more flat (Fig. 4F). Well developed Sharpey's fibres are visible near the parapophyses (Fig. 7B), on the ventro-lateral side of all the intercentra. These fibres are especially pronounced in the ventral cortex of the atlas (Fig. 4D), sacral and caudal intercentra (Fig. 7I).

Growth marks are visible only in the external part of cortex. Trabeculae deeper in the bone are usually destroyed and, thus, observations of any skeletochronological feature is difficult. In the outer cortex, the growth marks are represented by well developed, highly vascularised zones present in all specimens, except the smallest anterior dorsal (UOPB 00117). In two specimens (anterior dorsal UOPB 00115 and presacral UOPB 00118), the thin annulus without lines of arrested growth (LAGs) in the outermost cortex is visible. In two other specimens (atlas UOPB 00012 and the largest anterior dorsal UOPB 00114), closely spaced LAGs are recognised in the external annulus, four in the atlas and five in the anterior dorsal (Figs 4F, 6G).

2.2. Detailed histological description

2.2.1. Intercentrum of atlas. A transverse section of the atlas (UOBS 00859) reveals a thin periosteal cortex surrounding

https://doi.org/10.1017/S1755691013000273 Published online by Cambridge University Press

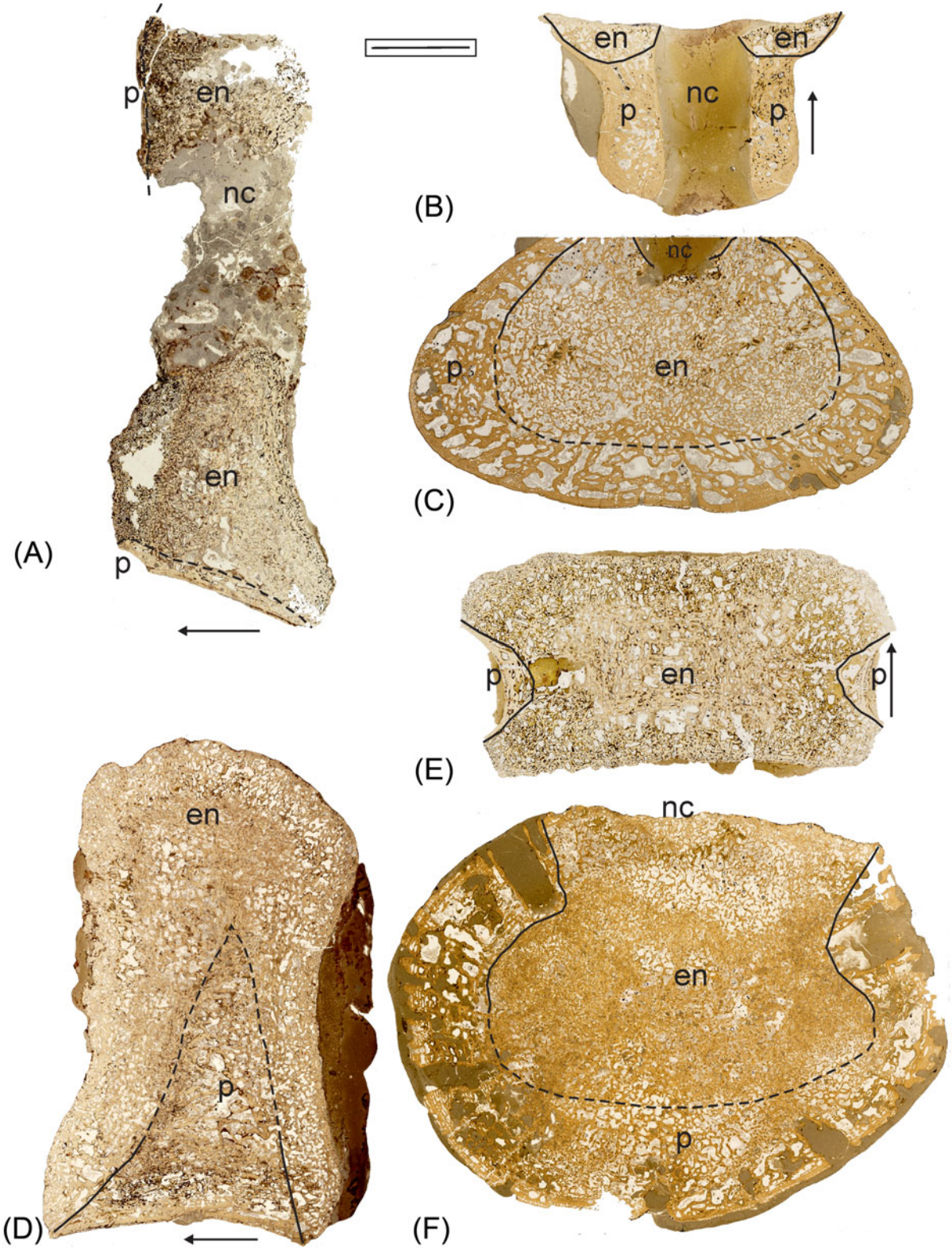

Figure 3 Microanatomy of vertebrae of *Metoposaurus diagnosticus krasiejowensis* from the Late Triassic of Poland: (A) sagittal section of the neural spine and intercentrum from the atlas UOPB 00012 (HOS4); (B) horizontal section of the basis of the neural arch from the atlas UOBS 00859 (HOS2); (C) transverse section of the intercentrum of the atlas UOBS 00859, on the dorsal side the floor of the neural canal. Note that, in this specimen, the clear periosteal part is thicker than in the previous specimen. It is linked with an intensive remodelling process in the subadult specimen, destroying the primary bone and rendering the primary border between the endochondrial and periosteal bone no longer visible; (D) sagittal section of the anterior dorsal intercentrum UOPB 00115 (HOS3); (E) horizontal section of the mid–dorsal intercentrum UOPB 01018 (HOS2). The determination of the ontogenetic stage in this plane is impossible; (F) transverse section of the presacral intercentrum UOPB 00118, on the dorsal side the floor of the neural canal. Black arrow indicates the anterior direction; continuous line shows the limit between the endochondral and periosteal bone (these bones show different orientations of their trabeculae: they are more regular and very sharp close to the ventral surface and around the neural canal in the periosteal bone); broken line shows the approximate limit between the endochondral and periosteal domains in the region of intensive remodelling. Abbreviations: en = endochondral bone; nc = sediment infill of the neural canal; p = periosteal bone. Scale bar = 1 cm.

https://doi.org/10.1017/S1755691013000273 Published online by Cambridge University Press

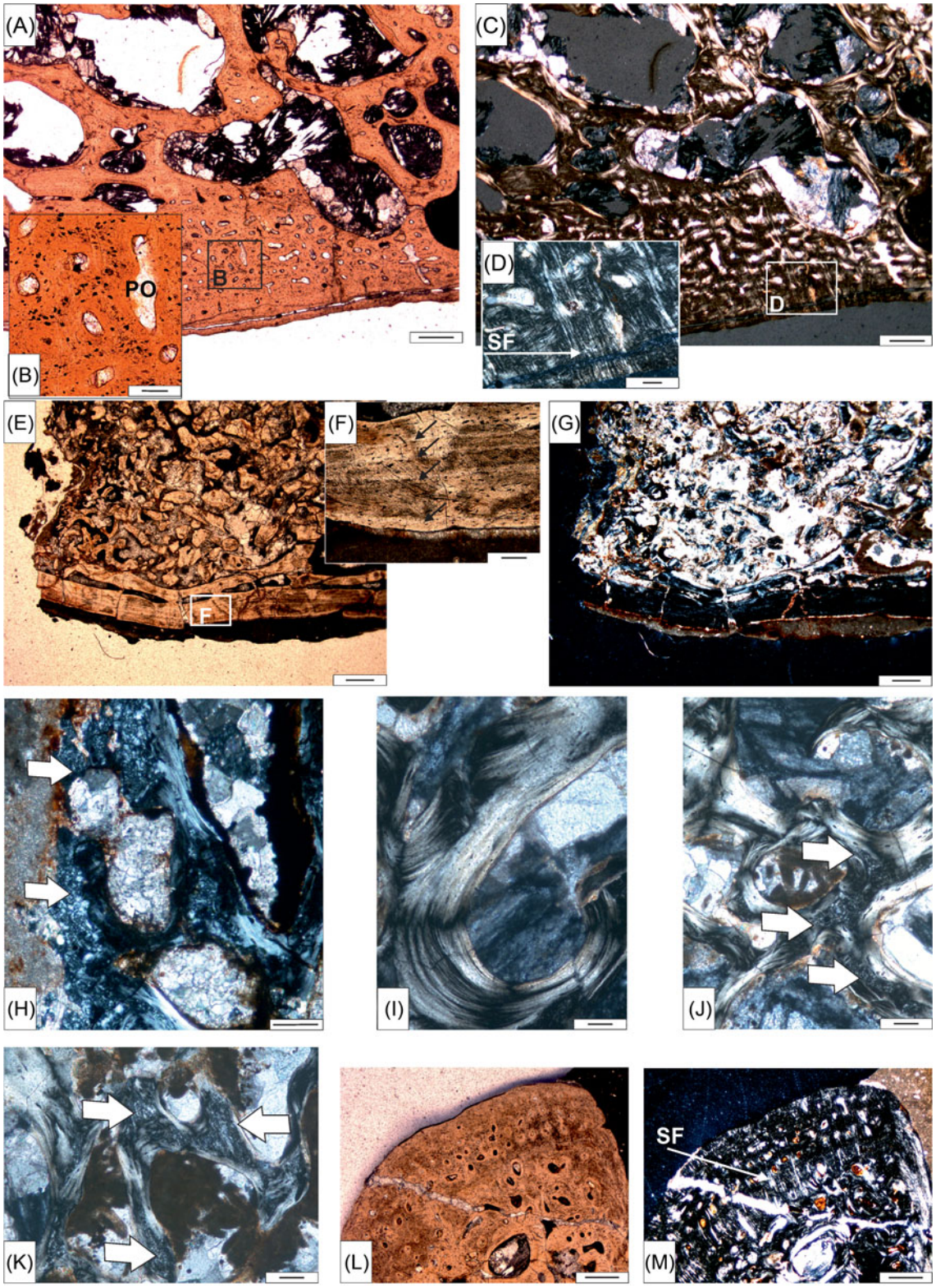

Figure 4 Histological section of atlases of *Metoposaurus diagnosticus krasiejowensis* from the Late Triassic of Poland. (A–D) transverse section of atlas UOBS 00859: (A) fragment of the periosteal cortex from the ventral side of the atlas UOBS 00859, in normal light; (B) close-up of (A) in normal light with primary osteons; (C) the same section as (A) in polarised light; (D) close-up of (C), the Sharpey's fibres are visible on the ventral side; image in polarised light. (E–G) sagittal section of the atlas UOPB 00012: (E) ventral part of atlas with visible thin cortex and endochondral trabeculae, image in normal light; (F) enlarged view of the external annulus with four LAGs (black arrows); (G) the same view as (E) in polarised light. (H) external layer of the cartilage (white arrows) on the articular face with the axis, visible in sagittal section of the atlas UOPB 00012; image in polarised light. (I) view of the secondary trabecular bone near the border between endochondral and periosteal bone with visible remodelling, transverse section form atlas UOBS 00859; image in polarised light. (J) more dorsal (as compared to I) part of endochondral domain with remains of calcified cartilage (white arrows) and the secondary trabeculae, transverse section from atlas UOPB 00859; image in polarised light. (K) peripheral part of the trabecular bone of the same specimen UOBS 00859 with numerous remains of calcified cartilage (white arrows) and thin trabeculae, in polarised light. (L–M) horizontal sections of the neural arch form atlas UOPB 00859 close to the intercentrum surface: (L) posterior part of the neural arch consisting of periosteal bone in normal light; (M) the same view as (L) in polarised light, with preserved Sharpey's fibres. All the transverse and sagittal sections are oriented with their ventral side towards the bottom of the figure. Abbreviations: SF = Sharpey's fibres, PO = primary osteons. Scale bars = 500 μm (A, C, E, G); 100 μm (B, D, F, H–M).

https://doi.org/10.1017/S1755691013000273 Published online by Cambridge University Press

the endochondral region, except in the small region of the neural canal. The endochondral region comprises most of the area of the thin-section (Figs 3C, 4A–D).

In the periosteal cortex, numerous vascular canals are present (Fig. 4A, B). In most cases, primary lamellar bone, forming primary osteons, is visible inside the vascular canals (Fig. 4B). Deeper in the cortex, large erosion cavities with secondary infilling are present (Fig. 4C). The matrix is derived from parallel-fibred bone. Osteocyte lacunae are numerous and round in shape (Fig. 4B).

In sagittal section (UOPB 00012), the periosteal cortex, only present in the ventral part (Figs 3A, 4E–G), is composed of two compact lamellar layers, with a single row of transverse-orientated vascular canals. In the external lamellar layer, four LAGs are observed (Fig. 4F). In the more internal cortex, the regular organisation of periosteal trabeculae decrease and remains of secondary trabeculae are observed, which gradually change into trabecular endochondral bone (Figs 3A, 4E–G).

The medullary region is composed exclusively of endochondral trabecular bone. Endochondral trabeculae are widely spaced. In the central part of the section, signs of remodelling are observed and secondary trabecular bone dominates (Fig. 4I). Closer to the dorsal, anterior and posterior surface, the amount of secondary bone decreases, the remains of calcified cartilage are numerous and primary endochondral trabecular bone is observed (Fig. 4J, K).

Large amounts of cartilage occur on the surface of the atlas, on the anterior (contacting the occipital condyles) and posterior (contacting the axis) sides (Fig. 4H). Abundant Sharpey's fibres are visible in the ventro-lateral region of the cortex (Fig. 4D).

2.2.2. Neural arch of atlas. In horizontal view, the shape of the base of the neural arch (from atlas UOBS 00859) is triangular, with a distinctive expanded anterior region (Fig. 3B). In the horizontal plane, almost the entire section is built of periosteal trabecular bone, with parallel-fibred organisation, except in the anterior part where the remains of endochondral bone are still visible (Fig. 3B). In this region, the primary endochondral trabecular bone is exposed to the surface. On the edge of this tissue, numerous remains of calcified cartilage are present. The primary endochondral trabecular bone changes gradually into periosteal bone through secondary trabecular bone. The lateral part of the base of the neural arch is built of periosteal bone with irregular rows of circular vascular canals, numerous erosion cavities located deeper in the bone, and almost an avascular layer near the surface. In the posterior region, three rows of longitudinal canals are present (Fig. 4L, M), along with numerous Sharpey's fibres (Fig. 4M). The central region is strongly remodelled, with large erosion cavities (Fig. 4L, M).

Similar to the intercentrum in sagittal view (UOPB 00012), weak development of trabecular bone is visible in the junction between the two upper parts of the neural arch. The avascular, thin cortex is present only on the anterior side (Fig. 3A).

2.2.3. Cervical region. The histology of one sampled post-cervical intercentrum (UOPB 01014, 38% of. max. estimated width) is similar to the general histological description of most vertebrae. In the transverse plane, the periosteal cortex is visible only in the ventral part of the section (Fig. 5A–D), below the parapophyses. Most of the cortex is highly vascularised, with primary lamellar bone inside canals, and parallel-fibred bone between them (Fig. 5B). Near the parapophyses, the cortex is less vascularised (Fig. 4C). The external, very thin layer of the cortex is more compact, avascular, and the organisation of collagen fibres is higher. Towards the central region of the section, the cortex is mostly destroyed but in preserved parts, the large erosion cavities are observed with intensive remodelling processes (Fig. 5A, D). Secondary trabecular bone, present near the endochondral-periosteal border (Fig. 5I), transforms gradually into endochondral trabeculae bone with numerous remains of calcified cartilage (Fig 5F–H).

2.2.4. Anterior dorsal intercentra. The comparison between thin-sections of the smallest, intermediate and the largest intercentra from the anterior-dorsal part of the axial skeleton shows a significant difference in the ossification degree of the endochondral trabecular bone and in the development of the cortex.

In the smallest intercentrum (UOPB 00117, 18% max. estimated width), the cortex is absent (Fig. 6A, B). The whole intercentrum is built only from endochondral trabecular bone, with remains of calcified cartilage (Fig. 6B). In larger specimens, a gradual development of the cortex is visible (Fig. 6C–H). In the medium in size UOPB 01010 (36% max. estimated width) intercentrum, the cortex is mostly destroyed. However, what remains of the cortex is a layer of highly vascularised, parallel-fibred bone with numerous but thin primary deposition of lamellar bone inside vascular canals, visible on the ventral side (Fig. 6C). In the specimen UOPB 00115 (47% max. estimated width), the primary deposition of lamellar bone in deeper vascular canals is thicker than in the previous slide. The thickness of the single trabecula is higher in the external region of the cortex. The matrix tissue in the external region is more lamellar than parallel-fibred, and formed the significantly thicker layer, termed annulus (Fig. 6D, E). In the largest specimen (UOPB 00114, 64% max. estimated size), further development of the external lamellar pattern is visible (Fig. 6F–H). In the most external annuli, five LAGs are present (Fig. 6G).

The endochondral region of the intercentra has a uniform structure with an irregular arrangement of the trabeculae and numerous remains of calcified cartilage. However, a gradual development of the remodelling process is observed. The smallest sample is dominated by primary endochondral bone, with large spaces in between trabeculae and numerous remains of calcified cartilage (Fig. 6B). However, near the ventral surface, the remodelling process and sparse secondary trabeculae are observed. In the largest specimen (UOPB 00114), the network of endochondral trabeculae is more dense, and the remodelling process more visible than in smaller samples. The remains of calcified cartilage are still present even in the central part of the intercentrum, which is dominated by secondary trabeculae. The amount of calcified cartilage is remarkably lower in the largest than in the smallest specimens. The remains of cartilage on the anterior, posterior and in the floor of the neural canal are visible in all sectioned bones. In the case of the smallest specimen, calcified cartilage is also present on its ventral surface (Fig. 6B).

2.2.5. Mid-dorsal intercentra. Intercentra of very similar size have been cut in the sagittal (UOPB 01017) and horizontal (UOPB 01018 and UOPB 01019) planes. In UOPB 01017 (40% max. estimated width), a highly vascularised cortex is present. In the horizontal plane at the level of the parapophyses, two to three rows of longitudinally orientated canals are observed in the lamellar-zonal bone, when visible (Fig. 7A, B). The bone matrix is organised into parallel fibres. In the vascular canals, primary lamellar bone is visible. Signs of resorption and secondary deposition of lamellar bone are present only in the deeper regions of the intercentrum.

In all sectioned mid-dorsal intercentra, the endochondral trabecular bone is weakly developed with thin trabeculae. Secondary bone predominates in the centre, while primary bone is more prominent towards the surface. Numerous remains of calcified cartilage are also present.

2.2.6. Presacral intercentrum. In the transverse plane of the presacral intercentrum (UOPB 00118, 83% of the max. width of the largest known from this position), the cortex is visible around the whole section, except near the neural canal

https://doi.org/10.1017/S1755691013000273 Published online by Cambridge University Press

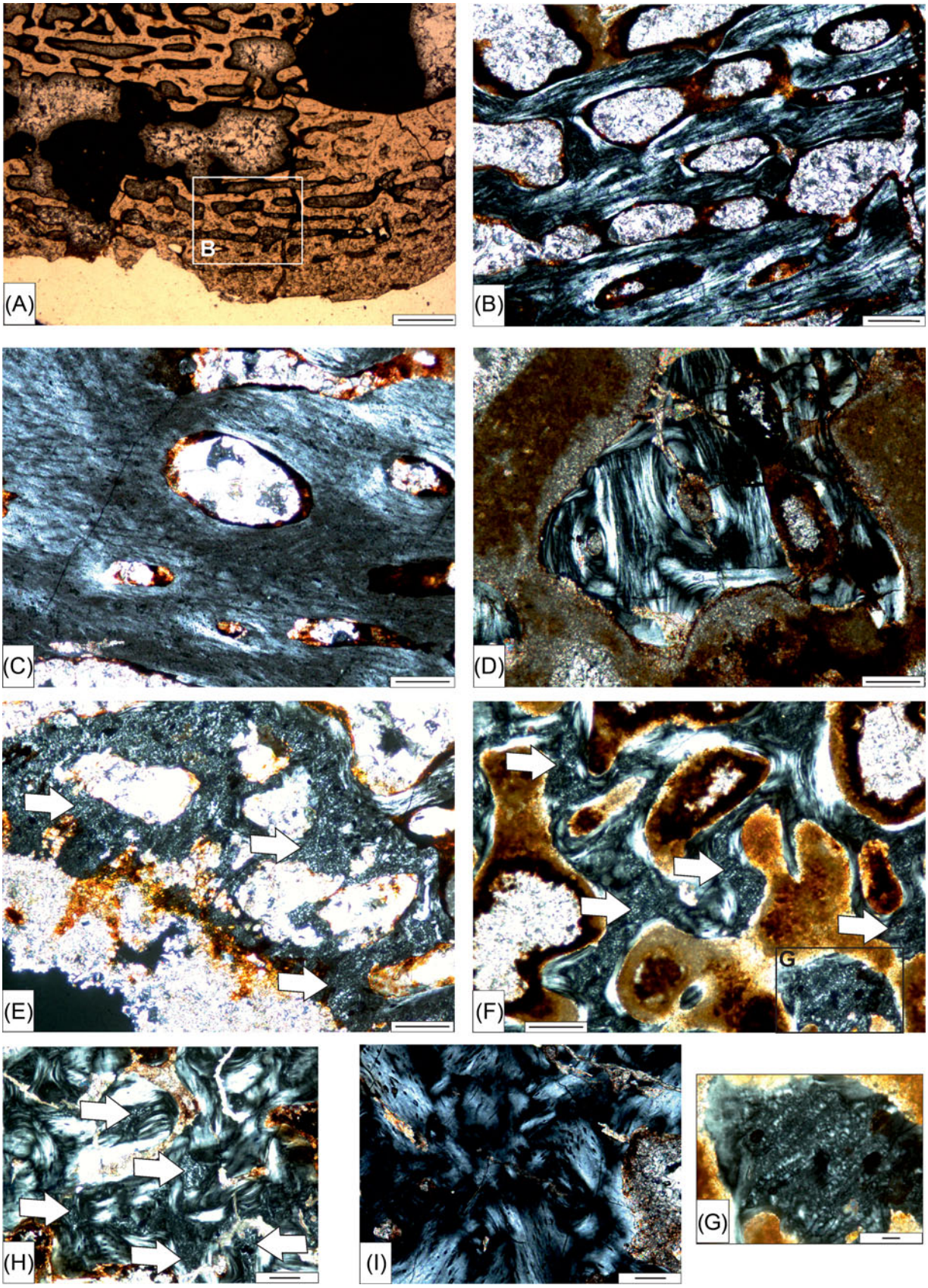

Figure 5 Histological, transverse section of the cervical intercentrum UOPB 01014 of *Metoposaurus diagnosticus krasiejowensis* from the Late Triassic of Poland: (A) ventral part of the cortex, in normal light; (B) highly vascularised cortex with primary deposition of the lamellar bone in the vascular canals, in polarised light; (C) less vascularised cortex from the parapophyses region, in polarised light; (D) cortex from the deeper region with remodelling, in polarised light; (E) layer of cartilage (white arrows) from the anterior surface, in polarised light; (F) primary endochondral trabecular bone with numerous remains of calcified cartilage (white arrows), in polarised light; (G) enlarged view of calcified cartilage from section F; (H) secondary trabecular bone with remains of calcified cartilage (white arrows), in polarised light; (I) strongly remodelled secondary trabecular bone from the central part of the section, in polarised light. Scale bars = 500 μm (A); 20 μm (G); 100 μm (B–F, H, I).

https://doi.org/10.1017/S1755691013000273 Published online by Cambridge University Press

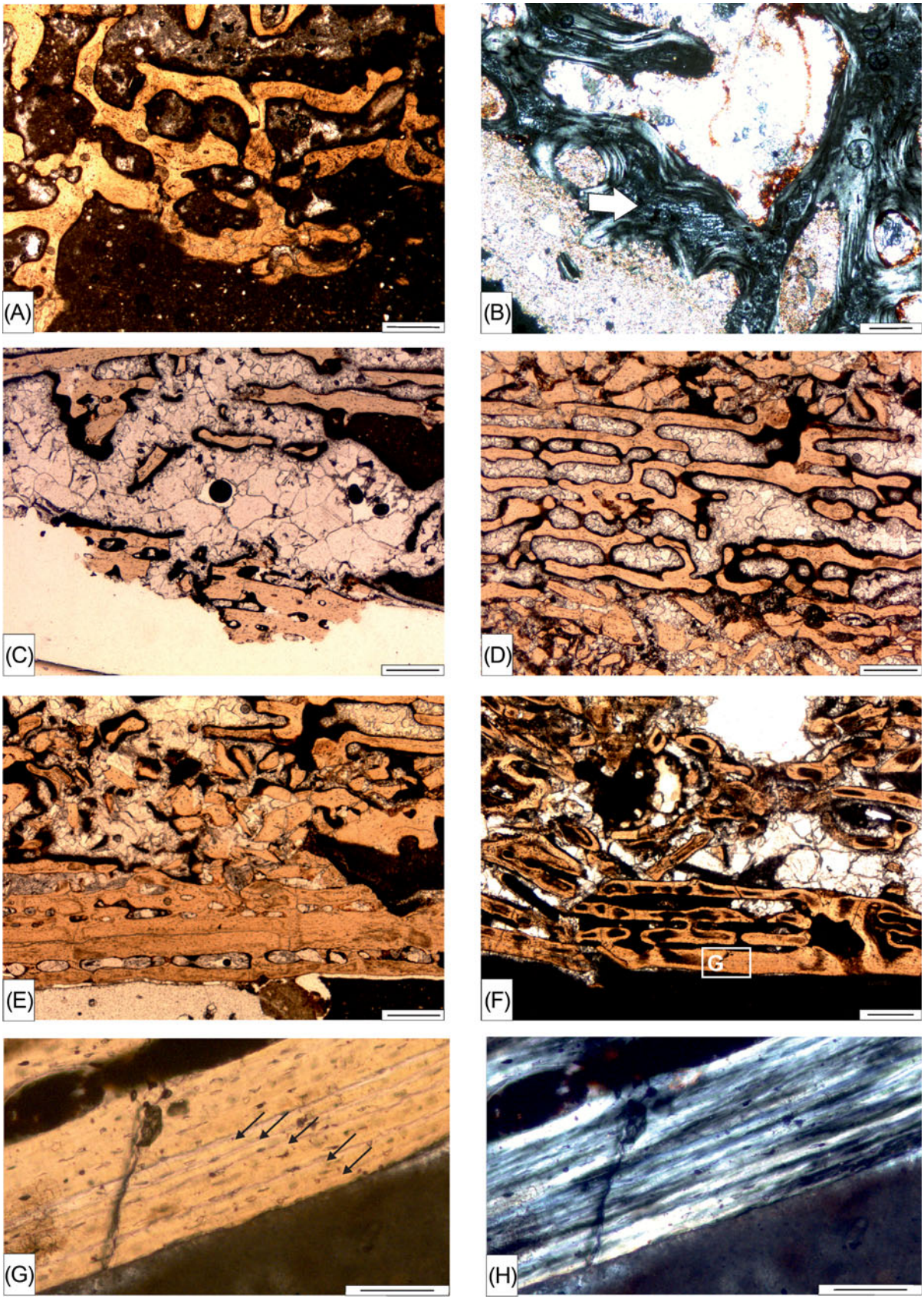

Figure 6 Sagittal sections of a growth series of anterior dorsal intercentra of *Metoposaurus diagnosticus krasiejowensis* from the Late Triassic of Poland: (A) cancellous bone in the ventral region of the early juvenile intercentrum UOPB 00117, image in normal light; (B) same view in polarised light with remains of calcified cartilage (white arrow); (C) ventral part of the juvenile anterior dorsal intercentrum UOPB 01010 in normal light; remains of the highly vascularised cortex visible in lower and upper part of image; (D) view of the deep region of a highly vascularised cortex from the late juvenile intercentrum UOPB 00115, in normal light; (E) external part of the cortex with more compact trabeculae in normal light; (F–H) section from the oldest intercentrum UOPB 00114: (F) the outer part of cortex in normal light; (G) enlarged view of the external annulus with five LAGs (black arrows); (H) same view as (G), in polarised light. Scale bar = 100 μm (B, G, H); 500 μm (A, C–F).

https://doi.org/10.1017/S1755691013000273 Published online by Cambridge University Press

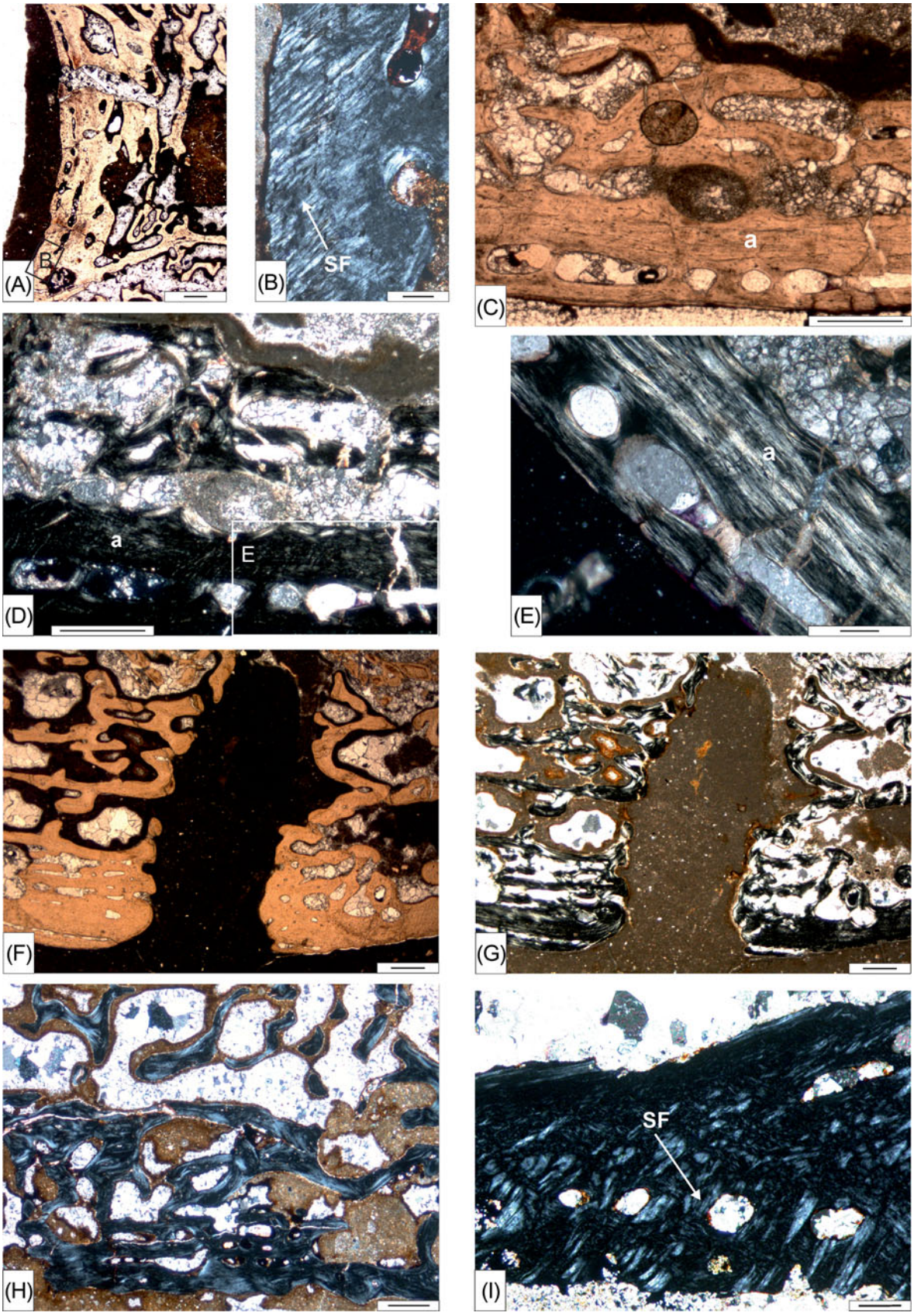

Figure 7 Histological sections of mid–dorsal, sacral and caudal intercentra of *Metoposaurus diagnosticus krasiejowensis* from the Late Triassic of Poland. (A–B) horizontal section of mid-dorsal intercentrum UOPB 01018: (A) cortex near the parapophyses, image in normal light; (B) close-up of (A) in polarised light, with visible Sharpey's fibres. (C–G) transverse section of presacral intercentrum UOPB 00118: (C) ventral cortex with large cavities on the periosteal surface; image in normal light; (D) same view as (C) in polarised light; (E) enlarged fragment of (D), with visible annulus with more organised collagen fibres; (F) periosteal surface with open cavity, image in normal light; (G) same view as (F) in polarised light. (H) thin ventral cortex (lower part) and trabecula from the anterior caudal intercentrum UOPB 01005 in sagittal section, image in polarised light. (I) cortex of the posterior–caudal intercentrum UOPB 01004, in transverse section; image in polarised light with visible Sharpey's fibres. Abbreviations: a = annulus; SF = Sharpey's fibres. Scale bars = 100 μm (B, E); 500 μm (A, C, D, F–I).

https://doi.org/10.1017/S1755691013000273 Published online by Cambridge University Press

in the dorsal region (Fig. 3F). The external part of the cortex is relatively poorly vascularised, with a lamellar matrix (Fig. 7C–E). Directly under the compact bone, large erosion cavities with secondary deposition of lamellar bone are present (Fig. 7D). The periosteal domain merges gradually into the endochondral region. The periosteal surface contains numerous, open cavities (Figs 3F, 7F, G). In the endochondral trabecular bone, a secondary type of deposition dominates in the central part of the intercentrum. Closer to the surface, numerous remains of calcified cartilage are also observed.

2.2.7. Postsacral intercentra. The histological pattern of the postsacral intercentra (UOPB 01008, UOPB 01011, respectively 84% and 92% of max. width of the largest know from this position) is similar to the previous sample. The cortex is present around the whole intercentrum in transverse sections, except on the floor of the neural canal. The bone is more compact near the parapophyses, and a very high vascularisation dominates the ventral side (Fig. 7H). The cortex, consisting only of lamellar bone, is extremely thin in the dorsal region, over the parapophyses. Similar to the previous sections, the periosteal surface is very porous.

2.2.8. Anterior and posterior caudal intercentra. The general histological pattern is similar in both types of intercentra (UOPB 01005 and UOPB 01004, respectively 92% and 73% of maximum width of the largest known from this position). In the sagittal section of the anterior intercentrum, the cortex is present only on the ventral side. It is well vascularised, with a thick deposition of lamellar bone inside. In the transverse section of the posterior caudal intercentrum, the cortex contains numerous vascular canals on the ventral side below the parapophyses, and it has one row of vascular canals between two layers of lamellar bone. In both cases, the secondary type of trabecular bone dominates the central region. Remains of calcified cartilage are visible on the dorsal side of both sections (where they are numerous between trabeculae) and on the anterior and posterior surfaces in sagittal section. On ventral side, the Sharpey's fibres are visible (Fig. 7I).

3. Discussion

3.1. Vertebral growth processes

3.1.1. Morphogenesis. Observations of a growth series of anterior-dorsal intercentra suggest a lengthwise growth (in the long axis). This process relies on endochondral ossification, ascertained by numerous remains of cartilage on both the anterior and posterior articular surfaces in all samples, independent of their size (Figs 4H, 5E).

In the dorso-ventral direction (height), both types of ossification (endochondral and periosteal) can be observed. On the dorsal side, in the region of the neural canal, only the endochondral ossification is present on all the sampled intercentra. On the ventral side, only the endochondral ossification initially occurs. It is well visible in the smallest specimen (UOPB 00117, 17% of max. estimated width), where the cortex is absent around the whole intercentrum (Fig. 6A, B). In the medium-sized specimen (UOPB 01010, 36% of max. estimated size), a layer of periosteal bone, with extremely numerous vascular canals, is present on the ventral side (Fig. 6C). As mentioned above, in the sagittal section of the intercentrum, the periosteal bone forms a triangle on the ventral region (Fig. 3D). The apex of the triangle corresponds to the beginning of the periosteal ossification, and the position of the apex indicates where exactly the periosteal growing process originated in the ventral part of the intercentrum. In this region, the remodelling process is also the most intense, and the limit between the endochondral and periosteal bone is missing, mostly replaced by secondary trabeculae (Fig. 3D). In the transverse section, the cortex gradually expands first, laterally to the parapophyses, and then to the dorsal side, toward the neural canal region.

Consequently, the width of the intercentrum also increases initially as a result of the endochondral ossification, and a periosteal cortex develops later.

The pattern of the periosteal trabecular bone, initially formed on the ventral side, resembles the fibro-lamellar bone known in large mammals and dinosaurs (Chinsamy-Turan 2005; Erickson 2005; Klein & Sander 2008; Sander *et al.* 2011), with the exception of the bone matrix found between numerous primary osteons (e.g. Fig. 4C). In typical fibro-lamellar bone, the bone matrix has a woven arrangement (Francillon-Vieillot *et al.* 1990), and usually the tissue suggests a rather rapid osteogenesis and a relatively fast growth rate (Amprino 1947; Margerie *et al.* 2002). Similarly, very highly vascularised parallel-fibred bone, instead of woven bone in the matrix, suggests rapid growth.

Here, the growth rate seems to decrease as the periosteal bone develops, and this is initially visible in the ventral cortex of UOPB 00115 (47% of max. estimated width). The structure of the whole cortex is mainly trabecular, but the thickness of a single trabecula of the outer region is significantly higher than in deeper cortex (Fig. 6C). Deep in the highly vascularised part of the cortex, on the ventral side of the largest intercentrum (UOPB 00114, 64% of max. estimated width), the remodelling process is greatly advanced. However, the trabecular organisation still dominates. The outermost region of the cortex contains a thick layer of trabeculae (Fig. 5D, E).

Interestingly, endochondral bone is present on the floor of the neural canal, which is contrary to what is normally observed in Amniota. In *Metoposaurus*, the vertebrae mainly consist of the intercentrum, whereas Amniota possess a pleurocentrum (Romer 1997). These two vertebral types have different origins leading to different histological organisation.

3.1.2. Interpretation of the ontogenetic stages. Formal histologic ontogenetic stages (HOS) erected by Klein & Sander (2008) have turned out to be of considerably heuristic value in discussing changes during ontogeny. Here, we present four HOS for the vertebral intercentra of *Metoposaurus*. Also, the histological analysis of the growth series of the anterior-dorsal intercentra can provide interesting information about ontogeny.

The HOSs are determined according to the pattern of the periosteal bone: HOS 1 typically lacks periosteal ossification; HOS 2 consists of a wide periosteal bone; HOS 3 shows a decrease in vascularisation in the external cortex; and HOS 4 has LAGs in external cortex. The closely spaced lines visible on the sections are located on the outermost part of an annulus. Other characters may help determine the ontogenetic stage. In younger forms, primary and relatively thin deposits dominate inside vascular canals, and then a gradual increase in the number of layers of lamellar tissue is observed (HOS 2 to HOS 3). The compactness of the bone seems linked with a primary deposition of lamellar bone inside the vascular canals. However, the remodelling process starts to be very intense in the oldest part of the cortex, resulting in an increase of the porosity of the periosteal tissue (HOS 4).

The position of the apex of the periosteal triangle related to the geometrical centre of the intercentrum may also provide information about the relative duration of the periosteal ossification: the lower the position of the apex, the shorter the time of ossification.

In trabecular bone, numerous remains of calcified cartilage and a varying degree of remodelling are visible. In younger specimens, a higher amount of calcified cartilage in the entire section is very characteristic, which is also accompanied with the dominance of primary trabecular bone. In older individuals,

https://doi.org/10.1017/S1755691013000273 Published online by Cambridge University Press

the amount of secondary trabecular bone increases in the centre of section, with a simultaneous decrease of cartilage. The primary bone still dominates near the periphery (Fig. 5F).

The smallest specimen (UOPB 00117) is about 17% of the maximum estimated width and 27% of the width of the largest known specimen (Table 1). The complete lack of cortex (Fig. 6A, B) therefore suggests an early juvenile stage (HOS 1).

In the next stage (HOS 2), the beginning of a rapid periosteal deposition is observed (Fig. 6C). The first wide, highly vascularised cortex may be interpreted as a first growth zone. The pattern of this zone suggests a very intensive growth. The intercentra, with its trabecular zone, may belong to a juvenile. Periosteal ossification begins later than 17% of maximal estimated size and earlier than 36% (the second smallest and second ontogenetic stage anterior dorsal intercentrum). The proxy size for the beginning of the periosteal ossification is about 21–25% of maximal estimated size.

The decreasing growth of the periosteal bone is marked by thick trabeculae near the external surface and is characteristic for a late juvenile (HOS 3). The region with a slower growth rate may be interpreted as an annulus (Fig. 6D, E).

The largest anterior-dorsal intercentrum (UOPB 00114) and the atlas (UOPB 00012) show a final trabecula, thicker than the previous one, in which five and four LAGs are counted, respectively (Figs 4F, 6G, H). This is the next ontogenetic stage (HOS 4). The histological characters (i.e. the presence of LAGs; thickness of the lamellar deposition in the vascular canals; the advanced remodelling process and the central position of the apex of the periosteal triangle in the anterior-dorsal) indicate an ontogenetic stage for both, which is older than the others. However, the determination of ontogenetic stage is very difficult in this case. If one LAG is the result of an annual cessation of growth (as hypothesised by Castanet *et al.* 1993; Sanchez *et al.* 2008), the accumulation of growth lines may indicate the external fundamental system (EFS) and, thus, corresponds to the animals reaching or approaching maximum size. Otherwise, the size is only 64% of the maximal estimated for anterior dorsal intercentrum and 46% for the atlas (Table 1). Moreover, in long bones of *Metoposaurus diagnosticus* from Krasiejów, the preliminary histological data show a specific histological framework with thick zones, but also with thick annuli with an accumulation of numerous rest lines (Konietzko-Meier 2011). The accumulation of the LAGs in the external annulus appears similar to the typical EFS, but the repetition of this structure in each annulus (not only in the external) suggests that it is a character typical for *Metoposaurus* annuli deposition and linked with the local climate (Konietzko-Meier & Klein 2013). The ontogenetic stage determination for both intercentra with HOS 4 is described simply as an older than late juvenile. How far this stage is from a pre-adult stage is impossible to define. Further studies are needed on the larger specimens to test the potential development of the periosteal bone.

The intercentra from the sacral and caudal regions, except the late juvenile pre-sacral (UOPB 00118), most likely belong to juvenile forms (Table 1).

3.2. Ontogenetic trajectory

The detailed ossification sequence of the postcranial skeleton is known in a few temnospondyls, mostly small- to medium-sized taxa such as *Sclerocephalus* (Boy 1974; Schoch 2003, 2010; Schoch & Witzmann 2009), *Onchiodon* (Boy 1990; Witzmann 2005; Schoch 2010), *Archegosaurus* (Witzmann 2006; Witzmann & Schoch 2006a; Schoch 2010), *Acanthostomatops* (Witzmann & Schoch 2006b), *Micromelerpeton* (Boy 1995; Schoch 2010), *Melanerpeton* (Schoch 2004) and *Apateon* (Schoch 2004, 2010; Fröbisch *et al.* 2007; Sanchez *et al.* 2010b) from the Late Carboniferous or/and the Early Permian of Germany. This is the second study of a histological growth series in a temnospondyl (for the first, see Steyer *et al.* 2004) but the first observed ontogenetic trajectory for vertebrae. Generally, the morphological analysis of the axial skeleton of temnospondyls shows a predominantly anterior to posterior sequence of ossification in postcranial elements, from head to tail, and indicates the neural arch ossified earlier than the intercentrum (Romer 1939; Boy 1974; Carroll *et al.* 1999; Fröbisch *et al.* 2010).

The results of this study confirm the sequence of ossification from head to tail. The thickness of the primary lamellar deposition in the vascular canals, the density of trabeculae, and the degree of remodelling of trabecular bone are much higher in both atlases than in the other vertebrae from the same HOS level (Table 1). Also, the amount of calcified cartilage between trabeculae is distinctively lower. Histological results also support the hypothesis of the earlier ossification of the neural arch (Fröbisch *et al.* 2010), but some comments are needed: the sequence of ossification is recorded in the atlas, where the neural arch is permanently fused with the intercentrum. The more ossified pedicel parts of the neural arch show a higher remodelling rate than that of the intercentrum, indicating an earlier ossification. However, in the apex of the neural spine, the amount of calcified cartilage and the development of the trabecular bone are similar to those of the intercentrum. This is well visible in the sagittal section of the specimen UOPB 00012. However, the section of the apex of the neural spine is difficult to interpret: the cartilage, visible in sagittal view, is the remnants of the junction of the left and the right half of the arch, rendering the interpretation of the ossification of the entire specimen quite impossible.

The analysis of a growth series from the anterior-dorsal part of the vertebral column provides information about the rate of ossification of the endochondral and periosteal domain. Preservation of calcified cartilage suggests that the director coefficient of ontogenetic trajectory for endochondral ossification of vertebra is slow. Conversely, the ossification process of the periosteal bone starts relatively late (approximately 21–25% of max. estimated size), but is very intensive.

3.3. Interpretation of the cartilage – immaturity, paedomorphosis or plesiomorphy

A high amount of cartilage and calcified cartilage is present in all sampled intercentra. The layers of almost continuous cartilage, covering the anterior and posterior surfaces of intercentra and the area of the ventral part of the neural canal (Figs 4H, 5E), suggest an increasing endochondral growth pattern in the anterior, posterior and dorsal directions.

The calcified cartilage within the trabecular bone represents an intermediate state in the endochondral bone formation, and may indicate incomplete growth and bone immaturity (Hunziker 1994; Cancedda *et al.* 1995; Erlenbacher *et al.* 1995; Bianco *et al.* 1998), confirming the juvenile age of most of the sampled intercentra.

However, in *Metoposaurus*, the cartilage is present not only in juvenile forms as an intermediate state during ossification (Figs 4K, 5F) but also in between secondary trabeculae (Fig. 5H). This may indicate a peadomorphic character in the histological framework.

Analysis of temnospondyl morphology suggests a paedomorphic, osteologically immature postcranial skeleton for the aquatic taxa, i.e. most of the dvinosaurians and stereospondyls (e.g. Pawley & Warren 2004). The morphogenetically immature taxa retain incomplete ossified articulation surfaces and lack enlarged processes for muscle attachments, even in the largest specimens. As suggested above, an exception is the ossification degree of the *Metoposaurus* vertebral intercentrum

which consists of a fully ossified disc, although the rest of the postcranial skeleton is immature (Pawley 2006).

The histological vertebral pattern shows different tendencies. The morphology of the long bones does not show a complete ossification, whereas in the histological pattern of a growth series of *Dutuitosaurus* femora, the calcified cartilage is never present even in the smallest bone (Steyer *et al.* 2004). In contrast, the metoposaurids' vertebrae look morphologically very mature (Dutuit 1976; Sulej 2007) but their histological features suggest the opposite conclusion. Even a relatively large intercentrum is histologically more immature than suggested by its morphological features. A paedomorphic process is suggested by the preservation of the calcified cartilage.

There is the third possibility that the preservation of the calcified cartilage is the plesiomorphic condition. However, in the absence of good ontogenetic series for several successive sister taxa, it is difficult to test this hypothesis.

4. Conclusion

For the first time, microscopic observations presented above provide in-depth information about the vertebral intercentra of a large temnospondyl amphibian, the Late Triassic *Metoposaurus diagnosticus*, plus the microanatomical and histological patterns, and variations along the vertebral column. The intercentra are uniform in their pattern and largely consist of cancellous bone. The cortex of the intercentra was built initially of the periosteal trabecular, and parallel-fibred bone with primary and secondary depositions of lamellar bone in numerous vascular canals. Later in ontogeny, the lamellar bone forming more compact trabeculae is deposited. Simultaneously, a remodelling process is also observed. The degree of development of the cortex depends on the individual ontogenetic stage. On the basis of the histological structure, four HOSs were erected. The periosteal ossification began as a very rapid deposition of highly vascularised parallel-fibered bone, and then continues as a slower annual deposition of lamellar bone. The endochondral part of the intercentrum is built of weakly developed primary or secondary (in central part) trabecular bone with numerous remains of calcified cartilage.

During morphogenesis of the vertebrae, the antero-posterior growth, as well as the development of the neural canal region, were realised as endochondral ossifications. The increase in the diameter of the intercentrum resulted from the endochondral growth and then from the periosteal ossifications in both lateral and ventral directions.

The maximum estimated size of the sampled vertebrae and the development of histological characters suggest that all the sampled bones belong to juvenile individuals. The described ontogenetic stages also allow analysis of the ossification sequence along the vertebral column, confirming the hypothesis of the ossification going from head to tail. Even in the largest specimen, remains of the calcified cartilage are still present in the vertebrae.

5. Acknowledgements

The authors acknowledge Olaf Dülfer, Katja Waskow (University of Bonn) and Michał Jankowiak (University of Poznań) for preparing thin-sections and Georg Oleschinski for morphological and microanatomical photos. We thank all reviewers (S. Werning and S. J. Steyer) and editors for all comments. We are grateful to Jessica Mitchell (University of Bonn) for improving the English.

The researchers were sponsored by the Deutche Forschungsgemeinschaft (DFG-Unit 533, Biology of the Sauropod Dinosaurs) and by the Polish Ministry of Science and Higher Education (3rd edition of program: Support of International Mobility of Researchers). The authors also thank the Self-Government of the Opole Voivodeship, Association Dinopark and Association Delta for financial support of excavation camps in Krasiejów.

6. References

Amprino, R. 1947. La structure du tissu osseux envisagée comme expression de differences dans la vitesse de l'acroissement. *Archives de Biologie* **58**, 315–30.

Bianco, P., Descalzi Cancedda, F., Riminucci, M. & Cancedda, R. 1998. Bone formation via cartilage models: the 'borderline' chondrocyte. *Matrix Biology* **17** (3), 185–92.

Boy, J. A. 1974. Die Larven der rhachitomen Amphibien (Amphibia, Temnospondyli; Karbon-Trias). *Paläontologische Zeitschrift* **48**, 236–48.

Boy, J. A. 1990. Über einige Vertreter der Eryopoidea (Amphibia: Temnospondyli) aus dem europäischen Rotliegend (?höchstes Karbon-Perm) 3. *Onchiodon. Paläontologische Zeitschrift* **64** (3/4), 287–312.

Boy, J. A. 1995. Über die Micromelerpetontidae (Amphibia, Temnospondyli). 1. Morphologie und Palaoökologie des *Micromelerpeton credneri* (Unter-Perm: SW Deutschland). *Paläontologische Zeitschrift* **69** (3/4), 429–57.

Buffrénil, V. de, Sire, J–Y. & Schoevaert, D. 1986. Comparaison de la structure et du volume squelettiques entre un delphinidé (*Delphinus delphi* L.) et un mammifère terrestre (*Panthera leo* L.). *Canadian Journal of Zoology* **64** (8), 1750–56.

Cancedda, R., Descalzi Cancedda, F. & Castagnola, P. 1995. Chondrocyte differentiation. *International Review of Cytology* **159**, 265–358.

Carroll, R. L., Kuntz, A. & Albright, K. 1999. Vertebral development and amphibian evolution. *Evolution and Development* **1** (1), 36–48.

Castanet, J., Francillon-Vieillot, H., Meunier, F.-J. & Ricqlès, A. de. 1993. Bone and individual ageing. *In* Hall, B. K. (ed.) *Bone*, 245–83. Boca Raton, Florida: CRC Press.

Chinsamy, A., & Raath, M. A. 1992. Preparation of bone for histological study. *Palaeontogia africana* **29**, 39–44.

Chinsamy-Turan, A. 2005. *The Microstructure of Dinosaur Bone: Deciphering Biology with Fine-scale Techniques*, 1–195. Baltimore: Johns Hopkins University Press.

Damiani, R. J. 2000. Bone histology of some Australian Triassic temnospondyl amphibians: preliminary data. *Modern Geology* **24**, 109–24.

Dutuit, J. M. 1976. Introduction à l'étude paléontologique du Trias Continental Marocain. Description de premiers Stégocéphales recueillis dans le Couloir d'Argana (Atlas Occidental). *Mémoires du Muséum National d'Histoire Naturelle Paris* **36**, 1–253.

Dzik, J., Sulej, T., Kaim, A. & Niedźwiedzki, R. 2000. Późnotriasowe cmentarzysko kręgowców lądowych w Krasiejowie na Śląsku Opolskim. *Przegląd Geologiczny* **48**, 226–35.

Dzik, J. & Sulej, T. 2007. A review of the early Late Triassic Krasiejów biota from Silesia, Poland. *Palaeontologia Polonica* **64**, 3–27.

Enlow, D. H. & Brown, S. O. 1956. A comparative histological study of fossil and recent bone tissues. I. *Texas Journal of Science* **8**, 405–43.

Erickson, G. M. 2005. Assessing dinosaur growth patterns: a microscopic revolution. *Trends in Ecology and Evolution* **20** (12), 677–84.

Erlebacher, A., Filvaroff, E. H., Gitelman, S. E. & Derynck, R. 1995. Toward a molecular understanding of skeletal development. *Cell* **80** (3), 371–78.

Francillon-Vieillot, H., de Buffrénil, V., Castanet, J., Géraudie, J., Meunier, F.-J., Sire, J.-Y., Zylberberg, L. & Ricqlès, A. de. 1990. Microstructure and mineralization of vertebrate skeletal tissues. *In* Carter, J. G. (ed.) *Skeletal Biomineralization: Patterns, Processes and Evolutionary Trends* **I**, 471–530. New York: Van Nostrand Reinhold.

Fröbisch, N. B., Carroll, R. L. & Schoch, R. R. 2007. Limb ossification in the Paleozoic branchiosaurid *Apateon* (Temnospondyli) and the early evolution of preaxial dominance in tetrapod limb development. *Evolution & Development* **9** (1), 69–75.

Fröbisch, N. B., Olori, J. C., Schoch, R. R. & Witzmann, F. 2010. Amphibian development in the fossil record. *Seminars in Cell and Developmental Biology* **21** (4), 424–31.

Gross, W. 1934. Die Typen des mikroskopischen Knochenbaues bei fossilen Stegocephalen und Reptilien. *Zeitschrift für Anatomie und Entwicklungsgeschichte* **203**, 731–64.

Hunziker, E. B. 1994. Mechanism of longitudinal bone growth and its regulation by growth plate chondrocytes. *Microscopy Research and Technique* **28** (6), 505–19.

Klein, N. & Sander, M. 2008. Ontogenetic stages in the long bone histology of sauropod dinosaurs. *Paleobiology* **34** (2), 247–63.

Konietzko-Meier, D. 2011. Seasonal-burrowing mode of life of *Metoposaurus diagnosticus krasiejowensis* (Amphibia, Temnospondyli) on the basis of osteohistological data. I International Symposium on Paleohistology. *Paleontologia i Evolució* **1**, 43.

Konietzko-Meier, D. & Klein, N. 2013. Unique growth pattern of *Metoposaurus diagnosticus krasiejowensis* (Amphibia, Temnospondyli) from the Upper Triassic of Krasiejów, Poland. *Palaeogeography, Palaeoclimatology, Palaeoecology* **370**, 145–57.

Margerie, E. de, Cubo, J. & Castanet, J. 2002. Bone typology and growth rate: testing and quantifying 'Amprino's rule' in the mallard (*Anas platyrhynchos*). *Comptes Rendus Biologies* **325** (3), 221–30.

Mukherjee, D., Ray, S. & Sengupta, D. P. 2010. Preliminary observations on the bone microstructure, growth patterns, and life habits of some Triassic temnospondyls from India. *Journal of Vertebrate Paleontology* **30** (1), 78–93.

Pawley, K. 2006. *The Postcranial Skeleton of Temnospondyls (Tetrapoda, Temnospondyli)*. PhD Thesis, La Trobe University, Melbourne, Australia. 422 pp.

Pawley, K. & Warren, A. A. 2004. Immaturity vs. paedomorphosis: A rhinesuchid stereospondyls postcranium from the Upper Permian of South Africa. *Paleontologica Africana* **40**, 1–10.

Ray, S., Mukherjee, D. & Bandyopadhyay, S. 2009. Growth patterns of fossil vertebrates as deduced from bone microstructure: case studies from India. *Journal of Biosciences* **34** (5), 661–72.

Ricqlès, A. de. 1975. Quelques remarques paléo–histologiques sur le problème de la néoténie chez les stégocéphales. *Colloques Internationaux du Centre National de la Recherche Scientifique* **218**, 351–63.

Ricqlès, A. de. 1976. Recherches paléohistologiques sur le os long des tétrapodes VII. Sur la classification, la signification fonctionnelle et l'histoire des tissus osseux des tétrapodes (Deuxième partie). *Annales de Paléontologie* (*Vértébres*) **62**, 71–126.

Ricqlès, A. de. 1978. Recherches paléohistologiques sur l'os long des tétrapodes VII. Sur la classification, la signification fonctionnelle et l'histoire des tissus osseux des tétrapodes (Deuxième partie). *Annales de Paléontologie* (*Vértébres*) **64**, 153–84.

Ricqlès, A. de. 1979. Relations entre structures histologiques, ontogenèse, strategies démographiques et modalités évolutives: le cas des reptiles captorhinomorphes et des stégocéphales temnospondyles. *Comptes Rendus de l'Académie des Sciences Paris* **288**, 1147–50.

Ricqlès, A. de. 1992. Paleoherpetology now: a point of view. *In*: Adler, K. (ed.) *Herpetology: current research on the biology of amphibians and reptiles. Proceedings of the First World Congress of Herpetology*, 97–120. Oxford, Ohio: Society for the Study of Amphibians and Reptiles.

Ricqlès, A. de., Castanet, J & Francillon–Vieillot, H. 2004. The "*message*" of bone tissue in paleoherpetology. *Italian Journal of Zoology* **1** (71), 3–12.

Romer, A. S. 1939. Notes on branchiosaurs. *American Journal of Science* **237**, 748–61.

Romer, A. S. 1997. *Osteology of the Reptiles*. Reprint edition. Malabar, Florida: Krieger Publishing Company. 722 pp.

Sanchez, S., Klembara, J., Castanet, J. & Steyer, J. S. 2008. Salamander-like development in seymouriamorph revealed by palaeohistology. *Biology Letters* **4** (4), 411–14.

Sanchez, S., Germain, D., Ricqlès, A. de, Abourachid, A., Goussard, F. & Tafforeau, P. 2010a. Limb–bone histology of temnospondyls: implications for understanding the diversification of palaeoecologies and patterns of locomotion of Permo–Triassic tetrapods. *Journal of Evolutionary Biology* **3** (10), 2076–90.

Sanchez, S., Ricqlès, A. de, Schoch, R. R. & Steyer, J. S. 2010b. Developmental plasticity of limb bone microstructural organization in *Apateon*: histological evidence of paedomorphic conditions in branchiosaurs. *Evolution and Development* **12** (3), 315–28.

Sanchez, S., Steyer, J. S., Schoch, R. R. & Ricqlès, A. de. 2010c. Palaeoecological and palaeoenvironmental influences revealed by long-bone palaeohistology: the example of the Permian branchiosaurid *Apateon*. *Geological Society, London, Special Publications* **339**, 139–49. Bath, UK: Geological Society Publishing House.

Sander, P. M., Klein, N., Stein, K. & Wings, O. 2011. Sauropod bone histology and its implications for sauropod biology. *In* Klein, N., K. Remes, K., Gee, C. T. & Sander, P. M. (eds) *Biology of the Sauropod Dinosaurs: Understanding the Life of Giants. Life of the Past* (series ed. J. Farlow), 276–302. Bloomington: Indiana University Press.

Schoch, R. R. 2003. The early larval ontogeny of the Permo-Carboniferous temnospondyl *Sclerocephalus*. *Palaeontology* **46** (5), 1055–72.

Schoch, R. R. 2004. Skeletal formation in the Branchiosauridae: a case study in comparing ontogenetic trajectories. *Journal of Vertebrate Paleontology* **24** (2), 309–19.

Schoch, R. R. 2010. Heterochrony: the interplay between development and ecology exemplified by a paleozoic amphibian clade. *Paleobiology* **36** (2), 318–34.

Schoch, R. R. & Witzmann, F. 2009. Osteology and relationships of the temnospondyl *Sclerocephalus*. *Zoological Journal of the Linnean Society* **157** (1), 135–68.

Steyer, J. S., Laurin, M., Castanet, J. & Ricqlès, A. de. 2004. First histological and skeletochronological data on temnospondyl growth: palaeoecological and palaeoclimatological implications. *Palaeogeography, Palaeoclimatology, Palaeoecology* **206**, 193–201.

Sulej, T. 2002. Species discrimination of the Late Triassic temnospondyl amphibian *Metoposaurus diagnosticus*. *Acta Palaeontologica Polonica* **47** (3), 535–46.

Sulej, T. 2007. Osteology, variability, and evolution of *Metoposaurus*, a temnospondyl from the Late Triassic of Poland. *Palaeontologia Polonica* **64**, 29–139.

Sulej, T. & Majer, D. 2005. The temnospondyl amphibian *Cyclotosaurus* from the Upper Triassic of Poland. *Palaeontology* **48** (1), 157–70.

Szulc, J. 2007. Keuper. *In* Szulc, J. & Becker, A. (eds) *Fieldtrip Guide, International Workshop on the Triassic of Southern Poland; Pan–European Correlation on the Epicontinental Triassic, 4th Meeting*, 5–6.

Wells, N. A. 1989. Making thin sections. *In* Feldmann, R. M., Chapman, R. E. & Hannibal J. T. (eds) *Paleotechniques*, 120–29. Knoxville: Department of Geological Sciences, University of Tennessee.

Witzmann, F. 2005. Hyobranchial and postcranial ontogeny of the temnospondyl *Onchiodon labyrinthicus* from Niederhäslich (Döhlen Basin, Autunian, Saxony). *Paläontologische Zeitschrift* **79** (4), 479–92.

Witzmann, F. 2006. Developmental patterns and ossification sequence in the Permo Carboniferous temnospondyl *Archegosaurus decheni* (Saar–Nahe Basin, Germany). *Journal of Vertebrate Paleontology* **26** (1), 7–17.

Witzmann, F. 2009. Comparative histology of sculptured dermal bones in basal tetrapods, and the implications for the soft tissue dermis. *Palaeodiversity* **2**, 233–70.

Witzmann, F. & Schoch, R. R. 2006a. The postcranium of *Archegosaurus decheni*, and a phylogenetic analysis of temnospondyl postcrania. *Palaeontology* **49** (6), 1211–35.

Witzmann, F. & Schoch, R. R. 2006b. Skeletal development of the temnospondyl Acanthostomatops vorax from the Lower Permian Döhlen basin of Saxony. *Transactions of the Royal Society of Edinburgh: Earth Sciences* **96** (4), 365–85.

Witzmann, F. & Soler–Gijón, R. 2010. The bone histology of osteoderms in temnospondyl amphibians and in the chroniosuchian *Bystrowiella*. *Acta Zoologica* (Stockholm) **91** (1), 96–114.

MS received 29 July 2011. Accepted for publication 11 December 2012.